# AXISYMMETRIC SELF-SIMILAR RUPTURE OF THIN FILMS WITH GENERAL DISJOINING PRESSURE

Michael Dallaston * [1], Dmitri Tseluiko[2], Serafim Kalliadasis[1], Zhong Zheng[3], Marco Fontelos[4], and Howard Stone[3]

[1]*Department of Chemical Engineering, Imperial College London, London, UK*

[2]*Department of Mathematical Sciences, Loughborough University, Loughborough, UK*

[3]*Mechanical and Aerospace Engineering, Princeton University, Princeton NJ, USA*

[4]*Departamento de Ciencia e Ingenieria, Universidad Rey Juan Carlos, Madrid, Spain*

*Summary* A thin film coating a dewetting substrate may be unstable to perturbations in the thickness, which leads to finite time rupture. The self-similar nature of the rupture has been studied by numerous authors for a particular form of the disjoining pressure, with exponent $n = 3$. In the present study we use a numerical continuation method to compute discrete solutions to self-similar rupture for a general disjoining pressure exponent $n$. Pairs of solution branches merge when $n$ is close to unity, indicating that a more detailed examination of the dynamics of a thin film in this regime is warranted. We also numerically evaluate the power law behaviour of characteristic quantities of solutions in the limit of large branch number.

## FORMULATION

A thin film on a dewetting substrate is dominated by the effects of surface tension and van der Waals forces. Invoking the *lubrication* or *thin film* approximation [3], the thickness of the film $h(\boldsymbol{x}, t)$ may be modelled by the (dimensionless) equation

$$\frac{\partial h}{\partial t} = -\nabla \cdot \left[h^3 \nabla \left(\nabla^2 h + \Pi(h)\right)\right], \qquad \Pi(h) = -\frac{1}{nh^n}. \tag{1}$$

As long as $n > 1$, the *disjoining pressure* $\Pi(h)$, which captures the effect of van der Waals forces, destabilises the film.This leads to finite time rupture, where $h$ vanishes at a point or line at time $t_0$. Assuming axisymmetry and self-similarity near a rupture point ($r = 0$), the film thickness may be expressed as $h(r, t) = (t_0 - t)^\alpha f(\xi)$, $\xi = r/(t_0 - t)^\beta$, where $f$ satisfies the following ordinary differential equation

$$-\alpha f + \beta \xi f' = -\frac{1}{\xi}\left[\xi f^3 \left(f'' + \tfrac{1}{\xi} f'\right)' + \xi f^{2-n} f'\right]', \quad f'(0) = f'''(0) = 0, \quad f \sim c\xi^{\alpha/\beta}, \, \xi \to \infty. \tag{2}$$

The similarity exponents $\alpha$ and $\beta$ are simple functions of the exponent $n$, while the far field condition is derived from the assumption of quasi-steadiness away from the rupture point. The conditions at $\xi = 0$ are required for symmetry and boundedness of the solution at the origin.

For $n = 3$, it has been shown that (2) has a discrete family of solutions, which may be characterised by the scaled film thickness at the origin $f_0 = f(0)$. Previously, these solutions have been computed numerically, using a shooting method [7], and Newton iteration on a discretised boundary value problem [5]. In each case, the numerical computation is highly sensitive to an initial guess (the right-hand initial condition for shooting, or the initial guess of the Newton scheme, respectively). The selection mechanism in the plane symmetry (line-rupture) version of (2) was explored in [1], where the exponential asymptotics of the large branch-number (equivalent to small $f_0$ was performed). The plane-symmetric version has also recently been resolved numerically [4] using the continuation algorithms implemented in the open source package AUTO07p [2].

The purpose of the present study is two-fold: firstly, we compute discrete solutions to (2) using numerical continuation, which has been shown to be highly effective on the plane-symmetric version of this problem [4]. Secondly, numerical continuation allows us to compute the discrete solution branches as the disjoining pressure exponent $n$ is varied.

## NUMERICAL CONTINUATION

The idea behind numerical continuation is to compute a solution to a boundary value problem that features a number of parameters, then gradually vary one or more of those parameters, using the previous solution as an initial guess (say, in a Newton iteration) to compute the new solution. The smooth dependence of the solution on parameters may thus be harnessed. The parameters in question may be model parameters, or *artificial parameters* introduced for numerical expediency, as we use here.

*Corresponding author. Email: m.dallaston@imperial.ac.uk

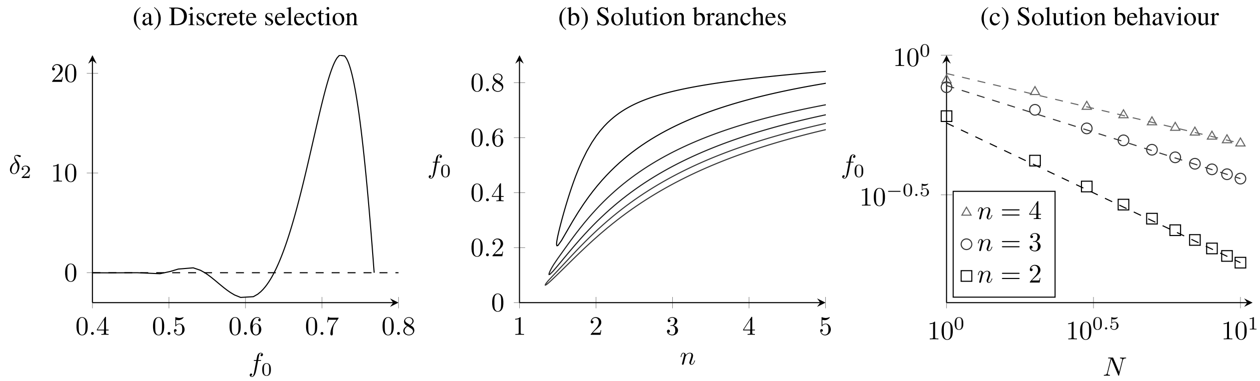


Figure 1: (a) The artificial parameter $\delta_2$ as a function of the scaled film thickness at the origin $f_0$; The roots $\delta_2 = 0$ correspond to solutions of (2). (b) The first six solution branches vs the disjoining pressure exponent $n$. Pairs of solution branches merge near $n = 1$. (c) Discrete solutions $f_0$ vs solution index $N$; solutions appear to asymptote to $\propto N^{-1/n}$ for large $N$.

As a starting point, we note that when $n = 3$, (2) has the exact solution $f_e(\xi) = c\sqrt{\xi}$ satisfying the far field conditions, but not the conditions at $r = 0$. We thus introduce the artificial parameters $\delta_1$ and $\delta_2$ into the boundary conditions, as well as an approximate left hand boundary location $\xi_0 \ll 1$, and enforce the conditions

$$f(\xi_0) = f_0, \qquad f'(\xi_0) = \delta_1, \qquad f'''(\xi_0) = \delta_2.$$

(the far field boundary conditions are also enforced at a large but finite value $\xi = L$). Given appropriate values of $\delta_1$ and $\delta_2$ , $f_e(\xi)$ also satisfies these boundary conditions, so may be used as an initial guess in our computation. Using numerical continuation, we now take $\delta_2$ and $\delta_1$ to zero, allowing $f_0$ to be free in each case. Now as $\xi_0$ is taken to zero, we approach a solution to the original problem (2).

The introduction of the artificial parameters also provides a systematic way of computing the other members of the discrete family of solutions. For $\delta_1 = 0$ and $\xi_0 > 0$ we allow $f_0$ to vary, letting $\delta_2$ be free. The curve of $\delta_2$ against $f_0$ oscillates around $\delta_2 = 0$, each intersection corresponding to a solution of (2). This approach is similar to that used for the plane symmetric problem [4], although in our case the variation of the artificial parameters in the boundary conditions cannot take place on $\xi = 0$ due to the coordinate singularity.

Finally, after finding the discrete solutions for $n = 3$, we continue in $n$ to trace out discrete solution branches.

## RESULTS

In figure 1a we plot the curve of the artificial parameter $\delta$ against $f_0$ for $n = 3$, showing the selection of discrete solutions where $\delta_2 = 0$. In figure 1b we plot the discrete branches of solutions, characterised by $f_0$, over a range of values of $n$. The most interesting phenomenon we observe is the merging of pairs of branches at a value $n > 1$ as $n$ decreases. Thus, for small values of $n$, the branch with largest $f_0$ (the only which is stable [5]) disappears. The dynamical behaviour of the time-dependent problem (1) in this regime is therefore of further interest, something which we intend to explore further by numerical computation of (1).

In addition we compute the relationship between $f_0$ on the discrete solution branches and the index $N$ of the branch (starting with the largest value as $N = 1$), particularly in the limit that $N$ is large. As shown in figure 1c, the discrete values of $f_0$ appear to behave as $\propto N^{-1/n}$ as $N \to \infty$ for $n = 3, 4$ and 5. When $n = 3$, the far field coefficient $c$ behaves as $N^{-0.43}$, as previously computed [6, 4]. The relationship between these numerically observed power laws, as well as the connection with the asymptotic result of [1], is ongoing work.

## References


[1] S. J. Chapman, P. H. Trinh, and T. P. Witelski. Exponential asymptotics for thin film rupture. *SIAM J. Appl. Math.*, 73(1):232–253, 2013.

[2] E. J. Doedel, A. R. Champneys, F. Dercole, T. F. Fairgrieve, Yu. A. Kuznetsov, B. Oldeman, R. C. Paffenroth, B. Sandstede, X. J. Wang, and C. H. Zhang. Auto-07p. *Continuation and bifurcation software for ordinary differential equations*, 2007.

[3] A. Oron, S. H. Davis, and S. G. Bankoff. Long-scale evolution of thin liquid films. *Rev. Mod. Phys.*, 69(3):931–980, 1997.

[4] D. Tseluiko, J. Baxter, and U. Thiele. A homotopy continuation approach for analysing finite-time singularities in thin liquid films. *IMA J. Appl. Math.*, 78(4):762–776, 2013.

[5] T. P. Witelski and A. J. Bernoff. Stability of self-similar solutions for van der Waals driven thin film rupture. *Phys. Fluids*, 11(9):2443–2445, 1999.

[6] T. P. Witelski and A. J. Bernoff. Dynamics of three-dimensional thin film rupture. *Physica D*, 147(1-2):155–176, 2000.

[7] W. W. Zhang and J. R. Lister. Similarity solutions for van der Waals rupture of a thin film on a solid substrate. *Phys. Fluids*, 11(9):2454–2462, 1999.